Theoretical study of electronic transport in monolayer SnSe

Sanjay Gopalan*, Gautam Gaddemane†[1], Maarten L. Van de Put‡, and Massimo V. Fischetti§
Department of Materials Science and Engineering
The University of Texas at Dallas, Richardson, Texas 75080
* Email: sanjay.gopalan@utdallas.edu
† Email: gautamg88@gmail.com
‡ Email: maarten.vandeput@utdallas.edu
§ Email: max.fischetti@utdallas.edu

***Abstract*—Monolayer SnSe is a two-dimensional (2D) material with an indirect band gap ($\sim$ 0.92 eV) that can be obtained relatively easily by exfoliating bulk SnSe crystals. Like most 2D van der Waals monolayers, its layered nature reduces or eliminates the defects found in bulk materials, such as surface interface roughness and dangling bonds. Here, we show promising results of first-principle calculations of the low-field mobility and high-field characteristics of monolayer SnSe by implementing the full-band Monte Carlo approach.**

***Keywords*—Monolayer SnSe, DFT, Monte Carlo, transport, mobility**

I. Introduction

The discovery of graphene has stimulated interest in two-dimensional materials, such as silicene [1]- [3], germanene [1]- [4], phosphorene [5]- [9] and transition metal dichalcogenides (TMDs) [10]- [16]. Monolayer SnSe has gained attention in VLSI applications, thanks to recent progress in growth techniques [17]- [18] and resulting in a low defect density [19] and in a promising measured carrier mobility [20]- [21].

Unfortunately, there are discrepancies in the intrinsic electron mobility calculated for monolayer SnSe. Shi *et al.* [22] performed a study of the transport properties of monolayer SnSe calculating the mobility within the deformation potential theory. They predicted the electron mobility in monolayer SnSe to be 757 $\mathrm{cm^2\,V^{-1}\,s^{-1}}$. However, the use of constant deformation potentials fails to account for the anisotropy of the matrix elements, leading to an overestimation of the mobility. Gaddemane *et al.* [5] have shown the importance of selecting the correct physical models and numerical approximations. For example, the lack of an accurate treatment often leads to an overestimation of mobility, as we suspect is the case in Ref. [22].

In order to clarify the situation, in this paper, we present a theoretical study of electronic-transport properties of monolayer SnSe. The band structure is calculated using density functional theory (DFT) as implemented in Quantum ESPRESSO (QE) [23] with the Perdew-Burke-Enzerhoff generalized-gradient approximation (GGA-PBE) [24] for the exchange-correlation functional, and the Optimized Norm-Conserving Vanderbilt (ONCV) [25] pseudopotential. The phonon spectrum is obtained using QE which employs density functional perturbation theory (DFPT). The electron-phonon scattering rates are calculated to first order using Fermi's golden rule. The electron-phonon Wannier (EPW) [26] code of the QE suite is used to calculate the electron-phonon matrix elements on a fine mesh in the first Brillouin Zone (BZ) by an interpolation strategy based on maximally-localized Wannier functions. Having obtained the electron-phonon scattering rates, we solve the Boltzmann Transport Equation (BTE) using a full-band Monte Carlo method. The Monte Carlo calculations for the low-field mobility calculations are performed assuming a zero electric field and estimating the electron mobility from the diffusion constant, using Einstein's relation. A uniform electric field is assumed when calculating the high-field behavior. A detailed description of the theoretical method is given in Ref. [1]

II. Results and Discussion

A. Band Structure and Phonon Spectrum

In Fig. 1, we show the calculated band structure of monolayer SnSe along the high-symmetry directions in the first BZ. Monolayer SnSe is an indirect band gap material with a band gap of 0.92 eV, with the conduction band minimum along the X-Γ (C_1 valley) direction and the valence band maximum along Y-Γ (C_2 valley) direction. We observe 5 satellite valleys ($C_1 - C_5$) in the first conduction band (see Fig.1) and the energy difference between each valley to conduction band minimum is given in Table 1. At present, there is disagreement about whether monolayer SnSe is a direct band gap or indirect band gap material as experimental investigations focusing on monolayer SnSe are scarce. Previous theoretical calculation done by Gomes *et al.* [27] found that SnSe is a direct band gap material. On the other hand, Guo et al. [28] have determined that it is an indirect band gap material. This difference stems from the discrepancy caused when using different 'flavors of DFT' which can be seen in 2D TMDs as studied by Gaddemane *et al.* [15]. From our calculations, we observe

This work has been supported in part by the Taiwan Semiconductor Manufacturing Company, Ltd (TSMC) and the Semiconductor Research Corporation (SRC-nCORE)

[1] Now at imec, Kapeldreef 75, 3001 Heverlee, Belgium

an energy difference between the direct and indirect band gap of 23 meV. Such a small energy difference between the conduction band minima along the Γ-X and Γ-Y directions in monolayer SnSe indicates that the semiconductor properties can be tuned from direct to indirect or vice versa by the application of external controls (*e.g.*, strain).

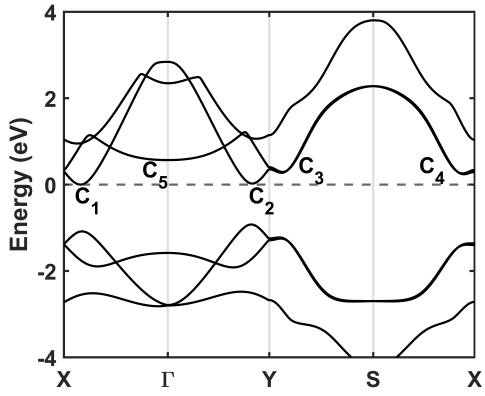

Fig. 1. Calculated band sturcture for monolayer SnSe along the high-symmetry directions of the first Brillouin Zone using the GGA-PBE exchange co-relational functionals

TABLE I
ENERGY DIFFERENCE BETWEEN CONDUCTION MINIMUM VALLEYS

Valleys	ΔE (meV)
$C_1 - C_2$	23
$C_1 - C_3$	272
$C_1 - C_4$	239
$C_1 - C_5$	567

Figure 2 illustrates the phonon dispersion of the 12 phonon branches that result from the presence of 4 atoms in the unit cell. The optical branches corresponding to the longitudinal optical phonons have a maximum frequency away from the Γ point in the BZ. This is a well-known phenomenon known as 'overbending' or 'Kohn anomaly' [29], which has been previously discussed in the case of monolayer h-BN [30] and monolayer InSe [16].

B. Scattering Rates

The density of states (Fig. 3), as well as the electron scattering rates (Fig. 4), are calculated and plotted as a function of electron kinetic energy (averaged over equi-energy surfaces). One can see a step-like increase in the density of states and electron scattering rates at about 25 meV and 560 meV. These steps are due to the onset of intervalley scattering between valleys C_1 and C_2 (at 25 meV) and between valleys C_1 and C_5 (at 560 meV). The intervalley scattering between other valleys cannot be distinguished as the interactions between them are weak.

C. Mobility and Velocity-field Characteristics

From the calculated diffusion constant, we obtain a low-field electron mobility of 72 $\mathrm{cm^2\,V^{-1}\,s^{-1}}$. This mobility is

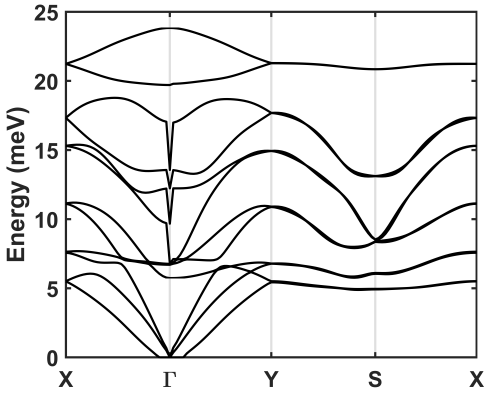

Fig. 2. Calculated phonon spectrum for monolayer SnSe along the high-symmetry directions of the first Brillouin Zone using the GGA-PBE exchange co-relational functionals

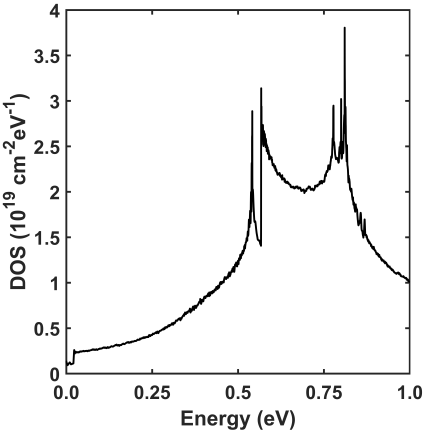

Fig. 3. Density of states plotted as a function of the electron energy with DFT calculations performed using the GGA-PBE functionals

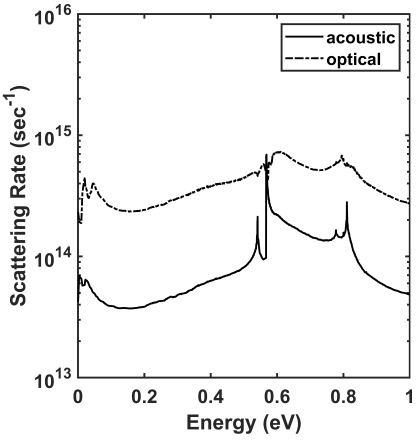

Fig. 4. The room-temperature (T = 300K) electron scattering rates plotted as a function of the initial electron energy (average over equi-energy surfaces) with DFT calculations performed using the GGA-PBE functionals

promising when compared to other widely studied 2D materials, such as phosphorene, silicene, and germanene. Finally, we have studied the velocity- and energy-field characteristics by assuming a homogeneous applied electric field along the zigzag direction [31]. The zigzag direction corresponds to Γ-X direction in k-space. We show, in Fig. 5a, with the dashed line, the drift velocity obtained from the mobility calculated from the diffusion constant.

Figure 6 shows the electron occupation in the first BZ. At low fields, the electrons populate only the regions near the conduction band minima at C_1 and C_2, as seen in Fig. 6a. However, at high fields, above 4×10^4 V/cm, the electrons become hot reaching an energy of 150 meV. However, due to low mobility when compared to bulk silicon, we do not observe the saturation of electron velocity at an electric field of 10^5 V/cm. Due to a significant increase of the average energy, the electrons in the C_1-valley gain enough energy to scatter to other valleys.

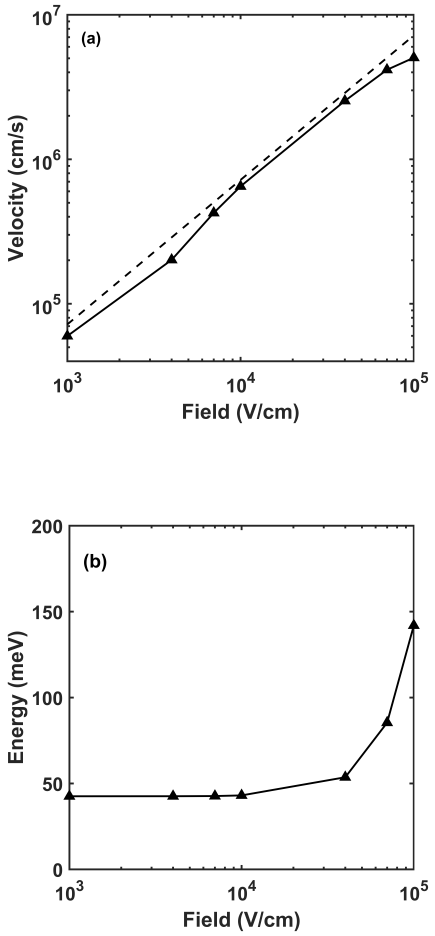

Fig. 5. (a) Velocity-field characteristics of monolayer SnSe and their corresponding (b) average energy-field plot at room temperature (T = 300K).

III. Conclusion

In an attempt to clarify the confusing situation regarding experimental and theoretical results regarding electron transport

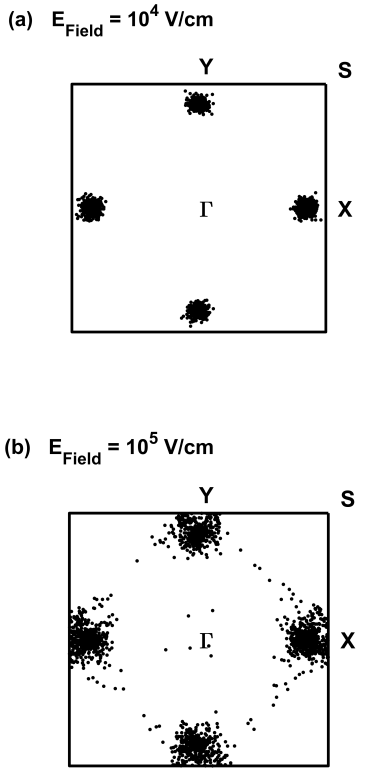

Fig. 6. Room temperature distribution of electrons in the first Brillouin Zone under the acceleration caused by a homogeneous electric field of strength.

in SnSe, we have performed DFT calculations as accurate as possible [1]. From these calculations we find a band gap of 0.92 eV, making this material suitable for complementary-logic applications. Using the full-band Monte Carlo method, we have calculated the low-field electron mobility and velocity-field characteristics of monolayer SnSe. We found an electron mobility of 72 $\mathrm{cm^2\,V^{-1}\,s^{-1}}$.

In order to assess the potential of monolayer SnSe as a candidate for a channel material in high-performance in field-effect devices, it is interesting to compare the intrinsic mobility of monolayer SnSe with the electron mobility of 1nm-thick Si slab. The calculated electron mobility of monolayer SnSe (72 $\mathrm{cm^2\,V^{-1}\,s^{-1}}$) exceeds the electron mobility of 1nm-thick Si (50 $\mathrm{cm^2\,V^{-1}\,s^{-1}}$), when accounting for surface roughness [32] under a transverse gate-field of 10^6 V/cm.

Considering the relatively large electron mobility we have obtained here and the recent progress in its growth techniques, monolayer SnSe should be viewed with interest for VLSI applications [33].

Acknowledgment

We acknowledge Dr. Edward Chen for his idea to study monolayer SnSe and also for his support.

REFERENCES

[1] G. Gaddemane, W. G. Vandenberghe, M. L. Van De Put, E. Chen, M. V. Fischetti, "Monte-Carlo study of electronic transport in non-σ_h-symmetric two-dimensional materials: Silicene and germanene," J. Appl. Phys., vol. 124, p. 044306, 2018.

[2] M. Houssa, E. Scalise, K. Sankaran, G. Pourtois, V. V. Afanas'ev, A. Stesmans, "Electronic properties of hydrogenated silicene and germanene," Appl. Phys. Lett., vol. 99, p. 223107, 2011.

[3] N. J. Roome and J. D. Carey, "Beyond graphene: Stable elemental monolayers of silicene and germanene," ACS Appl. Mater. Interfaces, vol. 6, pp. 7743-7750, 2014.

[4] M. E. Davila, L. Xian, S. Cahangirov, A. Rubio, G. L. Lay, "Germanene: A novel two-dimensional germanium allotrope akin to graphene and silicene," New J. Phys., vol. 16, p. 095002, 2014.

[5] G. Gaddemane, W. G. Vandenberghe, M. L. Van De Put, S. Chen, S. Tiwari, M. V. Fischetti, "Theoretical studies of electronic transport in monolayer and bilayer phosphorene: A critical overview," Phys. Rev. B., vol. 98, p. 115416, 2018.

[6] A. Castellanos-Gomez, L. Vicarelli, E. Prada, J. O. Island, K.L. Narasimha-Acharya, S. I. Blanter, D. J. Groenendijk, M. Buscema, G. A. Steele, J. V. Alvarez, et al. "Isolation and characterization of few-layer black phosphorus," 2D Mater., vol. 1, p. 025001, 2014.

[7] L. Li, Y. Yu, G. J. Ye, Q. Ge, X. Ou, H. Wu, D. Feng, X. H. Chen, Y. Zhang, "Black phosphorus field-effect transistors," Nat. Nanotechnol., vol. 9, pp. 372-377, 2014.

[8] H. Liu, A. T. Neal, Z. Zhu, Z. Lou, X. Xu, D. Tomanek, P. D. Ye, "Phosphorene: An unexplored 2D semiconductor with high hole mobility," ACS Nano., vol. 8, pp. 4033-4041, 2014.

[9] J. Qiao, X. Kong, Z. -H. Hu, F. Yang, W. Ji, "High-mobility transport anisotropy and linear dichroism in few-layer black phosphorus," Nat. Commun., vol. 5, p. 4475, 2014.

[10] A. Rawat, N. Jena, A. De Sarkar, "A comprehensive study on carrier mobility and artificial photosynthetic properties in group VI B transistion metal dichalcogenide monolayers," J. Mater. Chem., vol. A 6, pp. 8693-8704, 2018.

[11] T. Sohier, D. Campi, N. Marzari, M. Gibertini, "Mobility of two-dimensional materials from first principles in an accurate and automated framework," Phy. Rev. Mater., vol. 2, p. 114010, 2018.

[12] K. Kaasbjerg, K. S. Thygesen, K. W. Jacobsen, "Phonon-limited mobility in n-type single-layer MoS2 from first principles," Phy. Rev. B, vol. 85, p. 115317, 2012.

[13] Z. Jin, X. Li, J. T. Mullen, K. W. Kim, "Intrinsic transport properties of electrons and holes in monolayer transistion-metal dichalcogenides," Phy. Rev. B, vol. 90, p. 045422, 2014.

[14] W. Li, "Electrical transporrt limited by electron-phonon coupling from Boltzmann transport equation: An ab initio study of Si, Al, and MoS2," Phy. Rev. B, vol. 92, p. 075405, 2015.

[15] G. Gaddemane, S. Gopalan, M. L. Van de Put, M. V. Fischetti, "Limitations of ab inito methods to predict the electronic-transport properties of two-dimensional semiconductors: the computational example of 2H-phase transistion metal dichalcogenides," J. Comput. Electron, 2020. https://doi.org/10.1007/s10825-020-01526-1

[16] S. Gopalan, G. Gaddemane, M. L. Van de Put, M. V. Fischetti, "Monte Carlo study of electronic transport in monolayer InSe," Materials, vol. 12, no. 24, p. 4210, 2019.

[17] W. Shi, M. Gao, J. Wei, J. Gao, C. Fan, E. Ashalley, H. Li, Z. Wang, "Tin Selenide (SnSe): Growth, Properties, and Applications," Adv. Sci. vol. 5, no. 4, p. 1700602, 2018.

[18] T. Inoue, H. Hiramatsu, H. Hosono, T. Kamiya, "Heteroepitaxial growth of SnSe films by pulsed laser deposition using Se-rich targets," J. Appl. Phys., vol. 118, p. 205302, 2015.

[19] B. D. Tracy, X. Li, X. Liu, J. Furdyna, M. Dobrowolska, D. J. Smith, "Characterization of structural defects in SnSe2 thin films grown by molecular beam epitaxy on GaAs (111)B substrates," J. Cryst. Growth, vol. 453, p. 58, 2016.

[20] L.-C. Zhang, G. Qin, W. -Z. Fang, H. -J. Cui, Q. -R. Zheng, Q. -B. Yan, G. Su, "Tinselenidene: a Two-dimensional auxetic material with ultralow lattice thermal conductivity and ultrahigh hole mobility," Sci. Rep., vol. 6, p. 19830, 2016.

[21] L. B. Shi, M. Yang, S. Cao, Q. You, Y. Y. Niu, Y. Z. Wang, "Elastic behavior and intrinsic carrier mobility for monolayer SnS and SnSe: First-principles calculations," Appl. Surf. Sci., vol. 492, p. 435, 2019.

[22] L. -B. Shi, M. Yang, S. Cao, Q. You, Y. -Y. Niu, Y. -Z. Wang, "Elastic behavior and intrinsic carrier mobility for monolayer SnS and SnSe: First principles calculation," Appl. Surf. Sci., vol. 492, pp. 435-448, 2019.

[23] P. Giannozzi et al. "Quantum ESPRESSO: A modular and open-source software project for quantum simulations of materials," J. Phys. Condens. Matter, vol. 21, p. 395502, 2009.

[24] J. P. Perdew, Y. K. Burke, M. Ernzerhof, "Generalized Gradient Approximation made simple," Phy. Rev. B, vol. 88, p. 085117, 2013.

[25] D. R. Hamann, "Optimized norm-conserving Vanderbilt pseudopotentials," Phy. Rev. B, vol. 88, p. 085117, 2013.

[26] S. Ponce, E. R. Margine, C. Verdi, F. Guistino, "EPW: Electron-phonon coupling, transport and superconducting properties using maximally localized Wannier functions," Comput. Phys. Commun., vol. 209, pp. 116-133, 2016.

[27] L. C. Gomes and A. Carvalho, "Phosphorene analogues: Isoelectronic two-dimensional group-IV monochalcogenides with orthorhombic structure," Phys. Rev. B, vol. 92, p. 085406, 2015.

[28] S. -D. Guo and Y. H. Wang, "Thermoelectric properties of orthorhombic group IV-VI monolayers from the first-principles calculations," J. Appl. Phys., vol. 121, p. 034302, 2017.

[29] W. Kohn, "Image of the fermi surface in the vibration spectrum of a metal," Phy. Rev. Lett., vol. 2, p. 393, 1959.

[30] K. H. Michel, B. Verberck, "Theory of elastic and piezoelectric effects in two-dimensional hexagonal boron nitride," Phy. Rev. B, vol. 80, p. 224301, 2009.

[31] A. Shafique and Y. -H. Shin, "Thermoelectric and phonon transport properties of two-dimensional IV-VI compounds," Scientific Reports, vol. 7, p. 506, 2017.

[32] F. Gamiz and M. V. Fischetti, "Monte Carlo simulation of double-gate silicon-on-insulator inversion layers: The role of volume inversion," J. Appl. Phys., vol. 89, p. 5478, 2001.

[33] L. Li, Z. Chen, Y. Hu, X. Wang, T. Zhang, W. Chen, Q. Wang, "Single-Layer single-crystalline SnSe nanosheets," J. Am. Chem. Soc., vol. 135, no. 4, p. 1213, 2013.